Association of a History of Child Abuse With Impaired Myelination in the Anterior Cingulate Cortex: Convergent Epigenetic, Transcriptional, and Morphological Evidence

Pierre-Eric Lutz, M.D., Ph.D., Arnaud Tanti, Ph.D., Alicja Gasecka, Ph.D., Sarah Barnett-Burns, B.Sc., John J. Kim, B.Sc., Yi Zhou, B.Sc., Gang G. Chen, Ph.D., Marina Wakid, B.Sc., Meghan Shaw, B.Sc., Daniel Almeida, B.Sc., Marc-Aurele Chay, B.Sc., Jennie Yang, M.Sc., Vanessa Larivière, D.C.S., Marie-Noël M'Boutchou, M.Sc., Léon C. van Kempen, Ph.D., Volodymyr Yerko, Ph.D., Josée Prud'homme, B.Sc., Maria Antonietta Davoli, M.Sc., Kathryn Vaillancourt, B.Sc., Jean-François Théroux, M.Sc., Alexandre Bramoullé, M.Sc., Tie-Yuan Zhang, Ph.D., Michael J. Meaney, Ph.D., Carl Ernst, Ph.D., Daniel Côté, Ph.D., Naguib Mechawar, Ph.D., Gustavo Turecki, M.D., Ph.D.

Objective: Child abuse has devastating and long-lasting consequences, considerably increasing the lifetime risk of negative mental health outcomes such as depression and suicide. Yet the neurobiological processes underlying this heightened vulnerability remain poorly understood. The authors investigated the hypothesis that epigenetic, transcriptomic, and cellular adaptations may occur in the anterior cingulate cortex as a function of child abuse.

Method: Postmortem brain samples from human subjects (N=78) and from a rodent model of the impact of early-life environment (N=24) were analyzed. The human samples were from depressed individuals who died by suicide, with (N=27) or without (N=25) a history of severe child abuse, as well as from psychiatrically healthy control subjects (N=26). Genome-wide DNA methylation and gene expression were investigated using reduced representation bisulfite sequencing and RNA sequencing, respectively. Cell type–specific validation of differentially methylated loci was performed after fluorescence-activated cell sorting of oligodendrocyte and neuronal nuclei. Differential gene expression was validated using NanoString technology. Finally, oligodendrocytes and myelinated axons were analyzed using stereology and coherent anti-Stokes Raman scattering microscopy.

Results: A history of child abuse was associated with cell type–specific changes in DNA methylation of oligodendrocyte genes and a global impairment of the myelin-related transcriptional program. These effects were absent in the depressed suicide completers with no history of child abuse, and they were strongly correlated with myelin gene expression changes observed in the animal model. Furthermore, a selective and significant reduction in the thickness of myelin sheaths around small-diameter axons was observed in individuals with history of child abuse.

Conclusions: The results suggest that child abuse, in part through epigenetic reprogramming of oligodendrocytes, may lastingly disrupt cortical myelination, a fundamental feature of cerebral connectivity.

AJP in Advance (doi: 10.1176/appi.ajp.2017.16111286)

Child abuse is a major public health problem, affecting 5%–15% of all children in the Western world (1). Considerable clinical and epidemiological evidence shows that early-life adversity significantly increases the lifetime risk for stress-related psychiatric disorders, including depression and suicide. In particular, it has been suggested that this relationship may be mediated by various traits, including neuroticism (2), high levels of impulsivity and aggressive behaviors (3), and high anxiousness trajectories (4), which are typically observed in depressed individuals with a history of abuse. However, the neurobiological processes underlying this heightened vulnerability remain unclear.

Brain imaging studies have described brain network activity and structural abnormalities associated with child abuse, which may ultimately affect various aspects of cognitive and emotional processing (1). In particular, the anterior cingulate cortex, a critical region for the regulation of mood states, is among the brain areas most frequently associated with impairments in individuals with a history of child abuse. These include evidence of cortical thinning, alterations in network centrality and functional connectivity, and disruption of white matter integrity (reviewed in reference 1). While these studies bring invaluable insight into macrostructural adaptations associated with child

abuse, underlying cellular and molecular alterations are largely unknown.

Recently, epigenetic regulation of gene expression has emerged as a mechanism of long-term genomic plasticity that has the potential to explain how early experiences may drive behavioral changes over the lifetime (5). In particular, accumulating data suggest that patterns of DNA methylation, a major epigenetic mark, are progressively established during brain development and may be disrupted by early-life adversity (6). We therefore hypothesized that child abuse, by affecting the epigenetic programming of key developmental processes, may lead to long-term structural and functional changes that potentiate the vulnerability to psychopathology.

In the present study, focusing on the anterior cingulate cortex, we used a cohort of subjects with a history of severe child abuse (assessed through psychological autopsies [7]). We first performed genome-wide screenings of DNA methylation and gene expression and found that child abuse was associated with a severe disruption of oligodendrocyte function. We further demonstrated that part of the epigenetic adaptations in abused subjects selectively occurred in oligodendrocyte-lineage cells, but not in neurons. Notably, these effects were absent in depressed suicide completers with no history of child abuse, strongly suggesting that they are not accounted for by psychopathology. Furthermore, we provide evidence showing that offspring of dams with low maternal care, a well-investigated rat model of early-life environmental variation, present myelin gene expression changes that correlate with the effects of child abuse in humans.

Finally, associated cellular and subcellular changes were assessed using stereology and coherent anti-Stokes Raman scattering (CARS) microscopy, representing the first high-throughput analysis of individual myelinated axons in human subjects. The results demonstrate that child abuse selectively affects small-diameter axons and their myelin sheaths.

Altogether, our studies reveal with unprecedented resolution the impact of child abuse on the anterior cingulate cortex epigenomic and histopathological architectures, and unveil oligodendrocytes and myelination as potential major substrates mediating the long-term consequences of child abuse.

METHOD

Brain Samples

Anterior cingulate cortex tissue was obtained from the Douglas-Bell Canada Brain Bank from 1) subjects who died suddenly without prolonged agonal state or medical illness, and with no psychiatric history (control group); 2) subjects who died by suicide in the context of a major depressive episode and had a history of severe child abuse (child abuse group); and 3) subjects who died by suicide in the context of a major depressive episode and had no history of child abuse (depressed group). The groups were matched for age, postmortem interval, and brain pH (8) (see the data supplement that accompanies the online edition of this article). Psychological autopsies were performed as described previously

(9), with diagnoses assigned based on DSM-IV criteria. Characterization of early-life history was based on adapted Childhood Experiences of Care and Abuse interviews (10). We considered as severe adversity reports of nonrandom major physical and/or sexual abuse, up to age 15. Only cases with the maximum severity ratings of 1 and 2 were included. Histories of abuse were validated with available reports from medical charts, coroner files, or reports from youth protection services. Cingulate cortex tissue dissections and the rat model are described in the online data supplement.

Reduced Representation Bisulfite Sequencing (RRBS)

Libraries were prepared as described previously (see reference 11, the data supplement, and Table S1 in the data supplement).

Differential methylation. To identify differentially methylated regions, we used a windows approach defined by clusters of CG sites. Windows were defined using Bumphunter (http://bioconductor.org/packages/release/bioc/html/bumphunter.html) as any CG within 50 bp of another CG, with no limit on the number of CGs in a given window but with a minimum of two. The CGs included in differential methylation analyses were determined as follows: only CGs with ≥5X coverage were included; 2) only CGs informed in >15 subjects in each group were included; 3) for each subject contributing to a given window, at least two-thirds of the CGs in that window were informed; and 4) the 0.1% of CGs showing the highest coverage were discarded as potential polymerase chain reaction (PCR) amplification.

Fluorescence-Activated Cell Sorting (FACS)

Nuclei preparation. Frozen samples were homogenized, layered on a cushion of 0.8-M sucrose solution, and centrifuged at 2500 g (20 minutes at 4°C). Pellets were resuspended in blocking buffer containing primary antibodies against Sox10 (1:100; R&D Systems, Minneapolis) and NeuN (1:500; Alexa 700-conjugated; Novus, Littleton, Colo.). For the detection of Sox10+ nuclei, nuclei were incubated with a fluorophore-conjugated secondary antibody (Alexa Fluor 488, 1:500). Vybrant DyeCycle Violet stain was added to the nuclei solution.

Cell sorting. Using a FACSAria Fusion (BD Biosciences, San Jose, Calif.), a gating was applied to filter singlets using physical parameters and violet fluorescence (405-nm laser, 525/50 filter). Nonoverlapping gates were adjusted to collect neuronal nuclei based on NeuN-Alexa 700 immunoreactivity (640-nm laser, 730/45 filter), and oligodendrocyte nuclei based on Sox10-Alexa 488 immunoreactivity (488-nm laser, 530/30 filter).

Targeted Bisulfite Sequencing on FACS-Sorted Nuclei

DNA extractions. After overnight proteinase K digestion, samples were mixed with 770 μL of 20% PEG 8000 2.5-M NaCl and 200 μL of Agencourt AMPureXP Beads for every 200K nuclei. DNA extraction was subsequently conducted using a DynaMag-5 magnetic stand.

Library preparation. We used our PCR-based library preparation procedure (12) (see the online data supplement and Tables S2–S4). Libraries were quantified using an Agilent TapeStation, pooled, diluted to 8 pM, and sequenced on an Illumina MiSeq.

Bioinformatic analyses. After trimming universal primers, reads with a Phred quality score below 20 were discarded. Reads were aligned to the human genome hg19. CGs with a coverage lower than 10X were discarded.

RNA Sequencing

Only samples with RNA integrity numbers above 5 were used. Libraries were prepared at the Genome Quebec Innovation Center using the TrueSeq Stranded Total RNA Sample Preparation and Ribo-Zero Gold kits (Illumina) and quantified using PCR (KAPA Library Quantification). Three libraries were run per lane of an Illumina HiSEquation 2000 (100-bp paired-end), yielding ∼62 million reads/library (see Table S5 in the data supplement).

Differential expression analysis. We used FASTX-Toolkit and Trimmomatic for adapter trimming, TopHat (version 2.1.0) for alignment, and HTSeq-count for gene-level quantification. Differential expression was analyzed using DESeq2, and validations were conducted using reverse transcription PCR and NanoString.

Gene set enrichment analysis. As previously described (13), log_2 fold changes were obtained from the differential expression analysis. Genes were ranked based on fold changes. The GSEApreranked tool and the C2 curated gene sets were used.

CARS Microscopy

Frozen blocks of white matter adjacent to the anterior cingulate cortex were fixed in 10% formalin, and 300-μm thick sections cut on a vibratome. A custom-built video-rate laser scanning microscope and two laser sources were used to probe CH_2 stretching bands in myelin (2,845/cm). To extract nerve fiber morphometric information, a segmentation algorithm (14) was applied. For each fiber, standard morphometric measurements were computed from the segmentation results using MATLAB (MathWorks, Natick, Mass.).

Statistical Analysis

Differential methylation analysis (RRBS) was performed using a general linear model with age and gender as covariates and applying the Benjamini-Hochberg correction. For differential expression analysis (RNA sequencing), DESeq2 was used to perform general linear models with age, gender, and RNA integrity number as covariates. NanoString data were analyzed similarly with general linear models using child abuse and psychopathology as fixed factors. For DNA methylation in FACS-sorted nuclei, cellular densities after immunohistochemistry, and CARS morphometry analyses, one-way and two-way analyses of variance were used,

followed by Tukey's honest significant difference post hoc tests. The significance threshold was set to 0.05.

RESULTS

Epigenetic Effects of Child Abuse

Levels of DNA methylation were assessed with RRBS in the child abuse (N=27) and control (N=26) groups, covering on average 696,000 (SEM=40,000) CG dinucleotides per subject (see Figure S1 in the data supplement). Widespread differences were uncovered between groups (Figure 1A) (see also Figure S1E,F), and 115 genomic windows passed multiple-testing corrections (Benjamini-Hochberg, q<0.1). Among these, both hyper- and hypomethylation were detected in the child abuse group compared with the control group (see Figure S1F), suggesting that child abuse bidirectionally regulates epigenetic patterns in the cingulate cortex, as previously observed in the hippocampus (7). Strikingly, we noted that the three most significantly differentially methylated regions intersected with genes directly related to myelin and oligodendrocytes: LINGO3, of the LINGO family of proteins implicated in myelination (16); POU3F1, a transcription factor controlling myelination (17); and ITGB1, one of the integrins that mediate interactions between oligodendrocytes and axons (18).

Recent animal and human data suggest that DNA methylation patterns are cell type specific (6), and we therefore hypothesized that child abuse may selectively regulate oligodendrocytes through epigenetic processes. We conducted FACS sorting of nuclei from oligodendrocyte-lineage and neuronal cells (Figure 1B) (see also Figure S2 in the data supplement), using independent samples taken from adjacent tissue from the same subjects included in the RRBS study, and processed them through a targeted bisulfite sequencing analysis of DNA methylation in our top three RRBS differentially methylated regions. To control for the possible effects of depressive psychopathology and suicide, we included a third group of depressed individuals who died by suicide but had no history of child abuse (depressed group, N=25).

Interestingly, for both LINGO3 and POU3F1 (Figure 1C–H) (see also Figure S3 in the data supplement), decreased methylation in the child abuse group was confirmed and found to occur specifically in oligodendrocyte, but not neuronal, nuclei. These effects were absent in the depressed group. We found, however, no significant DNA methylation differences for ITGB1 in either Sox10+ or NeuN+ nuclei between groups.

Altogether, therefore, child abuse, but not suicide or depressive psychopathology, accounted for oligodendrocyte-lineage specific decreased DNA methylation in LINGO3 and POU3F1 genes, suggesting oligodendrocyte-specific epigenetic reprogramming as a result of child abuse.

Transcriptomic Effects of Child Abuse

We used RNA sequencing to further characterize genomic consequences of child abuse. Similar to the RRBS data, widespread differences were observed between the control and child abuse groups (see Figure S4E,F in the data

FIGURE 1. Epigenetic Adaptations in the Anterior Cingulate Cortex Following Child Abuse[a]
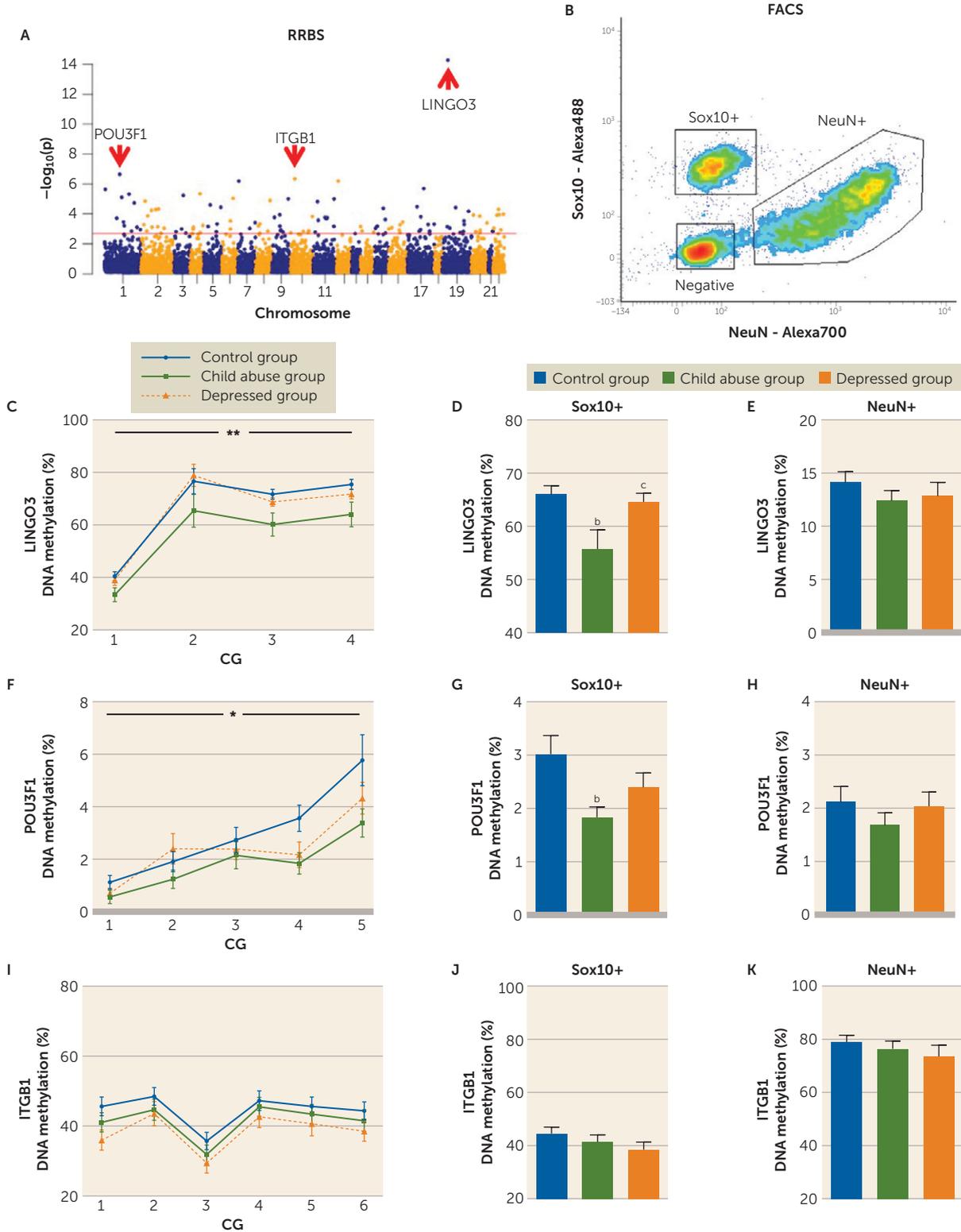
[a] Panel A is a Manhattan plot showing the genome-wide distribution of p values for all 5,724 windows between the child abuse group (N=27) and the control group (N=26). RRBS=reduced representation bisulfite sequencing. The red line indicates the threshold for genome-wide significance. Note that epigenetic adaptations associated with a history of child abuse are widespread along the genome. The top three windows showing the most significant differential methylation were located in genes related to myelin function, with decreased DNA methylation in the child abuse group for LINGO3 and POU3F1 and increased DNA methylation for ITGB1. Panel B illustrates the isolation of nuclei from neurons and oligodendrocytes using fluorescence-activated cell sorting (FACS). In panels C–K, DNA methylation was measured in sorted populations of NeuN+ and Sox10+ nuclei, focusing on differentially methylated loci identified by RRBS at the level of LINGO3, POU3F1, and ITGB1 genes. Error bars indicate standard error of the mean. After

supplement), with 3,734 differentially expressed genes (out of the 20,893 genes interrogated, i.e., 17.9% of p values <0.05 with no multiple testing correction). Compared with this genome-wide frequency, a list of 55 genes related to myelin and oligodendrocytes showed a strong enrichment for dysregulation (35/55, 63.6%) (see Figure S4F), which was confirmed by permutation testing ($p < 10^{-6}$) (see Figure S5 in the data supplement). Among these 55 genes, 32 genes were down-regulated and three up-regulated in the child abuse group (32/55 genes, Figure 2A–D). This enrichment for down-regulation was further confirmed by gene set enrichment analysis (enrichment score: −0.753; false discovery rate q<0.01) (Figure 2D). Down-regulations affected genes that are essential constituents of myelin (Figure 2A) and that critically control the synthesis of myelin lipids (Figure 2B) or the differentiation of oligodendrocytes (Figure 2C). Of note, this pattern of global down-regulation was absent in RNA sequencing data generated using tissue from the amygdala (see Figure S8 in the data supplement), suggesting that abuse-induced dysregulation of myelination may exhibit brain region specificity.

Focusing on the top differentially methylated genes identified by RRBS, we found that ITGB1 was strongly down-regulated in the child abuse group (Figure 2B), while the expression of LINGO3 (Figure 2B) and POU3F1 (Figure 2C) was not affected. Integrins are cell-cell interaction proteins, and numerous studies have shown that ITGB1, when expressed by oligodendrocytes, promotes myelination (18) by forming heterodimers with ITGA6 and ITGAV (20). Of note, the two latter genes were also down-regulated in the child abuse group (see Figure S7 in the data supplement), suggesting impaired communication between oligodendrocytes and nearby neurons or the extracellular matrix.

RNA sequencing results were validated using NanoString, and a strongly significant correlation was found between the two technologies (see Figure S4G). Notably, the global down-regulation of myelin genes was virtually absent in the depressed group (Figure 2E), suggesting that child abuse, but not depressive psychopathology, is specifically associated with impaired transcription of essential myelin genes.

To complement our findings, we used a well-established rodent model of maternal care (21) to measure how variation in early-life environmental experiences affects myelin in controlled experimental settings. We compared adult offspring of dams displaying high versus low levels of maternal behavior (high or low licking and grooming; see the data supplement) and quantified in the cingulate cortex the expression of the myelin-related genes that we observed differentially expressed in the human subjects as a function of child abuse. We observed a strong correlation (p<0.0001) between myelin gene expression changes in rats raised by low licking and grooming dams and expression changes in human subjects who had experienced child abuse (see Figure S9 in the data supplement). Although this model does not capture the whole spectrum of childhood abuse in humans, these results nevertheless strengthen the notion that myelin transcription is sensitive to the early-life environment.

Effects of Child Abuse on Oligodendrocyte Density
Genomic myelin alterations may reflect modifications in numbers of oligodendrocytes. Using stereology, we found that although the density of oligodendrocyte-lineage Sox10+ cells was similar between groups in the cingulate cortex gray matter (Figure 3B), compared with the control group it was significantly reduced in the cingulate cortex white matter of the child abuse group but not of the depressed group (Figure 3C).

In the adult brain, mature oligodendrocytes originate from oligodendrocyte progenitors. To investigate whether the effects of child abuse may stem from impaired proliferation in the oligodendrocyte lineage, we used the PDGFRα marker. We found that the density of PDGFRα+ cells was not different between groups (Figure 3C), suggesting that early-life adversity does not affect the proliferation of oligodendrocyte progenitors but reduces the pool of more mature myelinating oligodendrocytes in the cingulate cortex white matter.

Effects of Child Abuse on Myelin Ultrastructure
Molecular changes affecting myelin and associated with child abuse likely reflect the reduced number of oligodendrocytes observed in the cingulate cortex white matter of these


FACS, targeted bisulfite sequencing was used to generate high-coverage data in the control and child abuse groups as well as in a third group of depressed suicide completers who had no history of abuse (the depressed group, N=25). Comparison with the latter group was used to discard epigenetic adaptations potentially associated with psychopathology. In panels C−E, a group of four CGs showed decreased DNA methylation in the LINGO3 gene in the child abuse group that specifically occurred in the oligodendrocyte lineage (Sox10+ nuclei: two-way repeated-measures analysis of variance [ANOVA] [panel C]: group effect F=5.47, df=2, 72, p<0.01; CG sites effect, F=102.6, df=3, 216, p<0.0001; interaction F=0.51, df=6, 216, p>0.05; post hoc comparisons [panel D]: control group [N=24] versus child abuse group [N=26], p<0.01; child abuse group versus depressed group [N=25], p<0.05 by Tukey's honest significant difference] but not in neuronal [panel E] nuclei [NeuN+ nuclei: one-way ANOVA, F=0.89, df=2, 70, p>0.05). In panels F−H, a similar pattern was observed for POU3F1, with decreased DNA methylation in the oligodendrocyte-lineage (panels F−G) but not neuronal nuclei (panel H) of the child abuse group (Sox10+ nuclei: two-way repeated-measures ANOVA [panel F], group effect, F=4.81, df=2, 70, p<0.05; CG sites effect, F=24.8, df=4, 280, p<0.0001; interaction F=1.46, df=8, 280, p>0.05; post hoc comparisons [panel G]: control group [N=24] versus child abuse group [N=25], p<0.01; control group versus depressed group [N=24], p>0.05 by Tukey's honest significant difference). In panels I−K, we found no difference in ITGB1 methylation patterns between groups in either Sox10+ or NeuN+ nuclear fractions, suggesting that the differential methylation observed for this gene at the whole tissue level (using RRBS, panel A), which is further associated with decreased ITGB1 expression (see Figure 2), may occur in nonneuronal, nonoligodendrocyte cells. Of note, expression of ITGB1 by microglial cells has been reported (15) (two-way repeated-measures ANOVA [panel I], group effect, F=1.32, df=2, 65, p<0.27; CG sites effect, F=50.55, df=5, 325, p<0.0001; interaction F=0.77, df=10, 325, p>0.05).
[b] Control versus child abuse group, Tukey's honest significant difference, p<0.01.
[c] Child abuse versus depressed group, Tukey's honest significant difference, p<0.05.
*p<0.05. **p<0.01.

FIGURE 2. Transcriptomic Adaptations in the Anterior Cingulate Cortex Following Child Abuse[a]
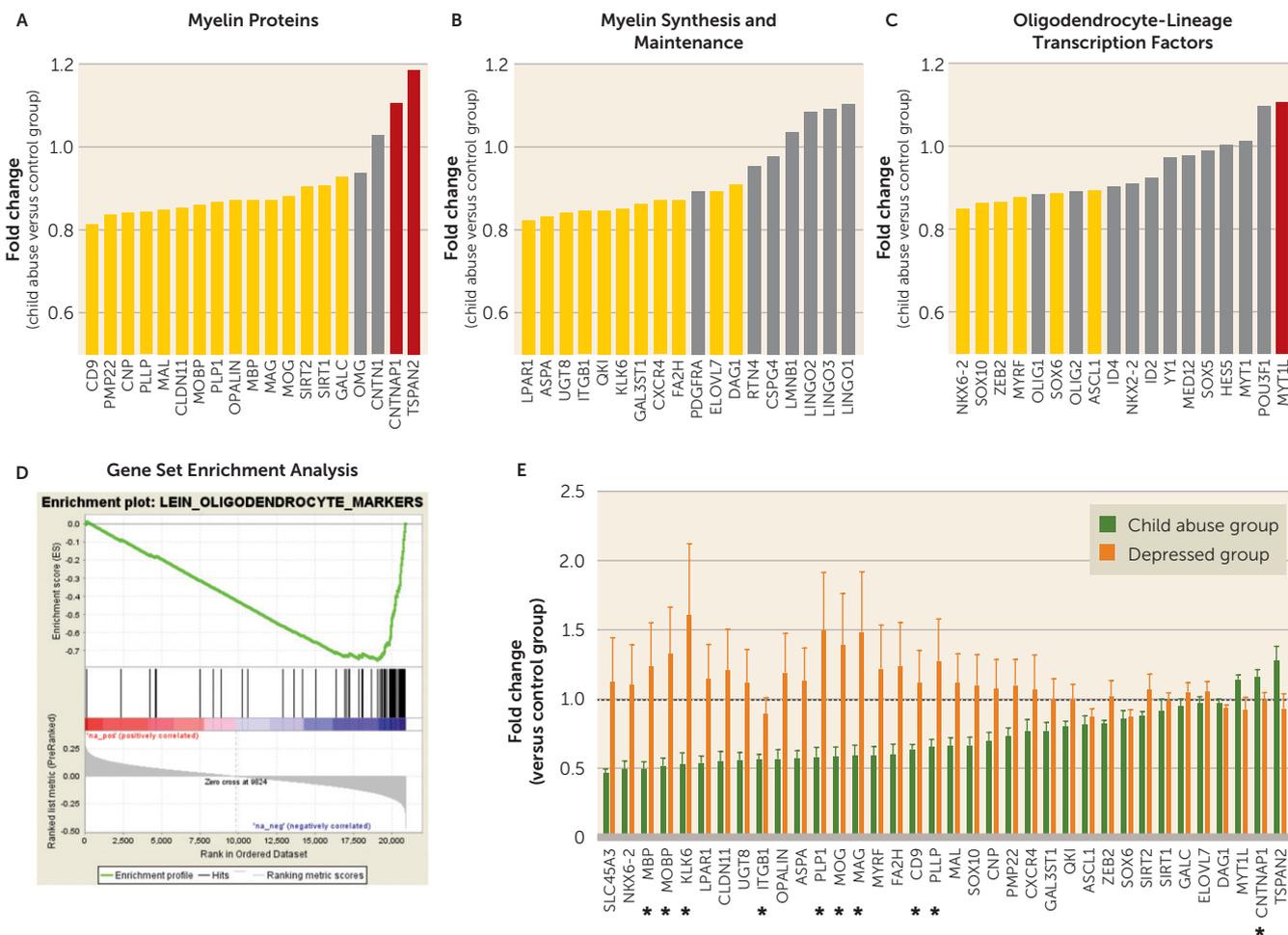
[a] In panels A–C, a literature-based list of 55 genes related to myelin or oligodendrocytes was used to interrogate RNA sequencing results (see also Figure S4F in the online data supplement). In the child abuse group, dysregulations were found for genes that are essential components of myelin sheaths (panel A), that allow for the synthesis of myelin phospholipids and myelin maintenance (panel B), and that specify the oligodendrocyte transcriptional program (panel C). Yellow and red bars indicate genes that were down- and up-regulated, respectively ($p < 0.05$). Panel D illustrates results of gene set enrichment analysis (GSEA): a collection of genes specifically expressed by oligodendrocytes previously established in the mouse brain (19) was enriched for genes showing evidence of down-regulation as a function of child abuse, with an enrichment score of -0.753 ($p < 0.0001$, false discovery rate $q < 0.01$). In panel E, NanoString technology was used for the validation of myelin dysregulation in the child abuse group compared with the control group, focusing on the 32 genes that were down-regulated and the three genes that were down- and up-regulated in RNA sequencing data, and using the same RNA samples as in RNA sequencing. A strongly significant correlation was found between RNA sequencing and NanoString fold changes (Pearson linear regression, $r^2 = 0.87$, $p < 0.0001$), with fold changes defined here as the ratio between groups, with the control group as the denominator (see Figure S4G in the data supplement). The expression of myelin genes was also measured in the group of depressed suicide completers who did not have a history of child abuse (depressed group, N=14). A general linear model was used to explore potential effects of child abuse and psychopathology and revealed significant effects of child abuse for 10 genes (asterisks): CNTNAP1 ($F=6.73$, df=1, 61, $p=0.012$), ITGB1 ($F=4.69$, df=1, 61, $p=0.034$), MOBP $F=5.04$, df=1, 61, $p=0.028$), PLP1 ($F=5.09$, df=1, 61, $p=0.028$), KLK6 ($F=4.81$, df=1, 61, $p=0.032$), MAG ($F=4.46$, df=1, 61, $p=0.039$), MOG ($F=4.33$, df=1, 61, $p=0.042$), PLLP ($F=4.30$, df=1, 61, $p=0.042$), MBP ($F=4.27$, df=1, 61, $p=0.043$), and CD9 ($F=4.05$, df=1, 61, $p=0.049$). In contrast, we found no significant effect of depressive psychopathology for any of the 35 genes examined, indicating that child abuse is specifically associated with impaired transcription of genes that are essential for myelin physiology. Fold changes correspond to ratios between groups, with control subjects as the denominator.

individuals. To explore whether these changes may affect myelin integrity and abundance, we conducted a high-throughput morphometric analysis of myelin using CARS microscopy (Figure 4A–C) (25). We implemented this technique for its use in human brain tissue (see Figure S10A–C and Table S10 in the data supplement), and analyzed a total of 18,949 axonal fibers with similar cross-sectional orientations. As expected, axonal diameter was significantly correlated with g-ratio, the commonly used myelination index (Figure 4D) (see also Figure S12 in the data supplement).

The results showed a moderate but significant decrease in axonal diameter in the child abuse group (Figure 4E) compared with the two other groups. Furthermore, in agreement with the down-regulation of myelin genes described above, we measured a decrease in average myelin thickness that was specific to the child abuse group (Figure 4F). Finally, we found that the g-ratio was significantly higher in the child abuse group (Figure 4G). Altogether, the decrease in axon diameter associated with child abuse was accompanied by an even stronger decrease in myelin thickness, resulting in an increased g-ratio (Figure 4H). These

FIGURE 3. Altered Densities of Oligodendrocyte-Lineage Cells in the Anterior Cingulate Cortex Following Child Abuse[a]
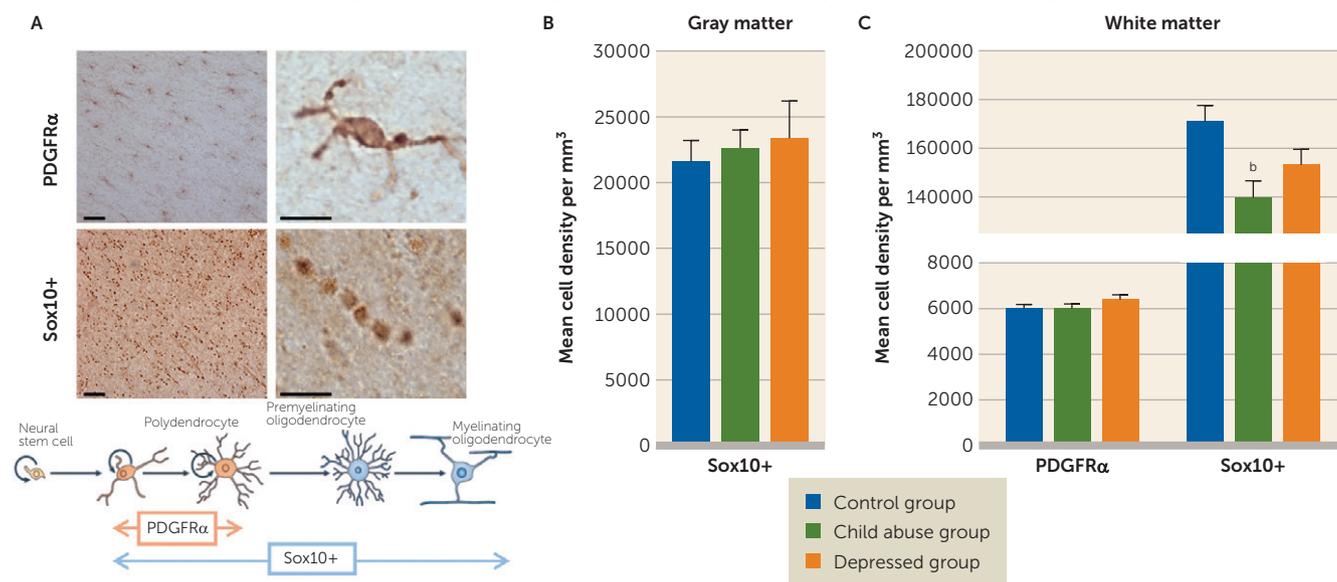
[a] Panel A shows representative images of oligodendrocyte progenitor cells and oligodendrocyte-lineage cells in the human postmortem cingulate cortex stained for PDGFRα and Sox10. The scale bars are 50 μm in the left panels and 10 μm in the right panels. Modified from reference 22. In panel B, densities of Sox10+ oligodendrocytes are similar in the cingulate cortex gray matter of control subjects (N=10), depressed suicide completers with a history of child abuse (child abuse group, N=6), and depressed suicide completers with no history of abuse (depressed group, N=7) (one-way analysis of variance [ANOVA], F=0.22, df=2, 20, p>0.05). Panel C shows densities of oligodendrocyte progenitor cells (PDGFRα+ cells) and oligodendrocyte-lineage cells (Sox10+ cells) in the white matter of the cingulate cortex. Compared with the control group, the child abuse group had a lower density of Sox10+ cells (one-way ANOVA: F=4.55, df=2, 24, p<0.05; post hoc comparisons: control subjects [N=6] versus child abuse subjects [N=10], p<0.05 by Tukey's honest significant difference; control subjects versus depressed subjects [N=11], p>0.05 by Tukey's honest significant difference), while no difference between groups was found for the density of PDGFRα+ cells (one-way ANOVA: F=1.31, df=2, 57, p>0.05), suggesting that decreased gene expression of oligodendrocyte-related transcription factors (e.g., Sox10 [23], Nkx6-2 [24]) observed in abused subjects (see Figure 2C) was associated with lower survival in this cell lineage. Error bars indicate standard error of the mean.
[b] Control versus child abuse group, Tukey's honest significant difference, p<0.05.

results suggest that both axonal morphology and myelination are affected by early-life adversity.

Axon caliber and myelin sheath thickness are tightly regulated properties that reflect the length, conduction velocity, and firing rate of individual fibers (26), as well as their neuroanatomical localization (27). To gain deeper insight into the impact of child abuse on myelination, we categorized fibers by axonal diameter. Notably, the two smallest-caliber categories (0.5–1.25 μm), encompassing more than 50% of all fibers, showed reduced myelin thickness specifically in the child abuse group (Figure 4K). Accordingly, the g-ratio was increased in the child abuse group for these two categories (Figure 4L), indicating that early-life adversity preferentially affects small-diameter axons in the cingulate cortex. Finally, we note that child abuse was also associated with increased diameter in the largest axons (>1.75 μm, Figure 4J), which likely correspond to long-range subcortical connectivity of the anterior cingulate cortex (28). We speculate that the latter changes, which do not have an impact on the g-ratio of these fibers, may nevertheless alter functional coupling between the cingulate cortex and subcortical structures such as the amygdala and nucleus accumbens and contribute to altered emotional processing in abused subjects.

DISCUSSION

MRI studies have suggested that early-life adversity may be associated with structural alterations in white matter (1). A recent report further provided evidence that interventions, such as placement in high-quality foster care, may partly counteract some of these effects, suggesting that white matter deficits could be reversed to alleviate lifelong consequences of early-life adversity (29). MRI technologies, however, offer limited specificity and spatial resolution: changes in diffusion tensor imaging fractional anisotropy, for example, may be related to changes in myelination, axonal number, axonal diameter, gliosis, or tissue edema (30). Most recent MRI strategies are able to more specifically interrogate myelin content (31), but they still only allow, at best, characterization of bundles of hundreds or thousands of axons. Here, we used state-of-the-art microscopy to precisely measure microstructural changes associated with early-life adversity. Our results provide direct evidence that axonal integrity and myelination of individual fibers may be disrupted in adults who have a history of abuse during childhood. Importantly, they suggest that this phenomenon predominantly affects small-diameter axons, possibly corresponding to cortico-cortical projections (32), while leaving other axonal populations unaffected. We propose that these selective myelin adaptations may provide a microstructural explanation for white matter defects previously detected by brain imaging studies of child abuse.

Beyond white matter myelin dysregulation, our results indicate that early-life adversity is also associated with profound epigenetic and transcriptomic alterations that

FIGURE 4. Child Abuse Decreases Myelination of White Matter Fibers in the Anterior Cingulate Cortex[a]
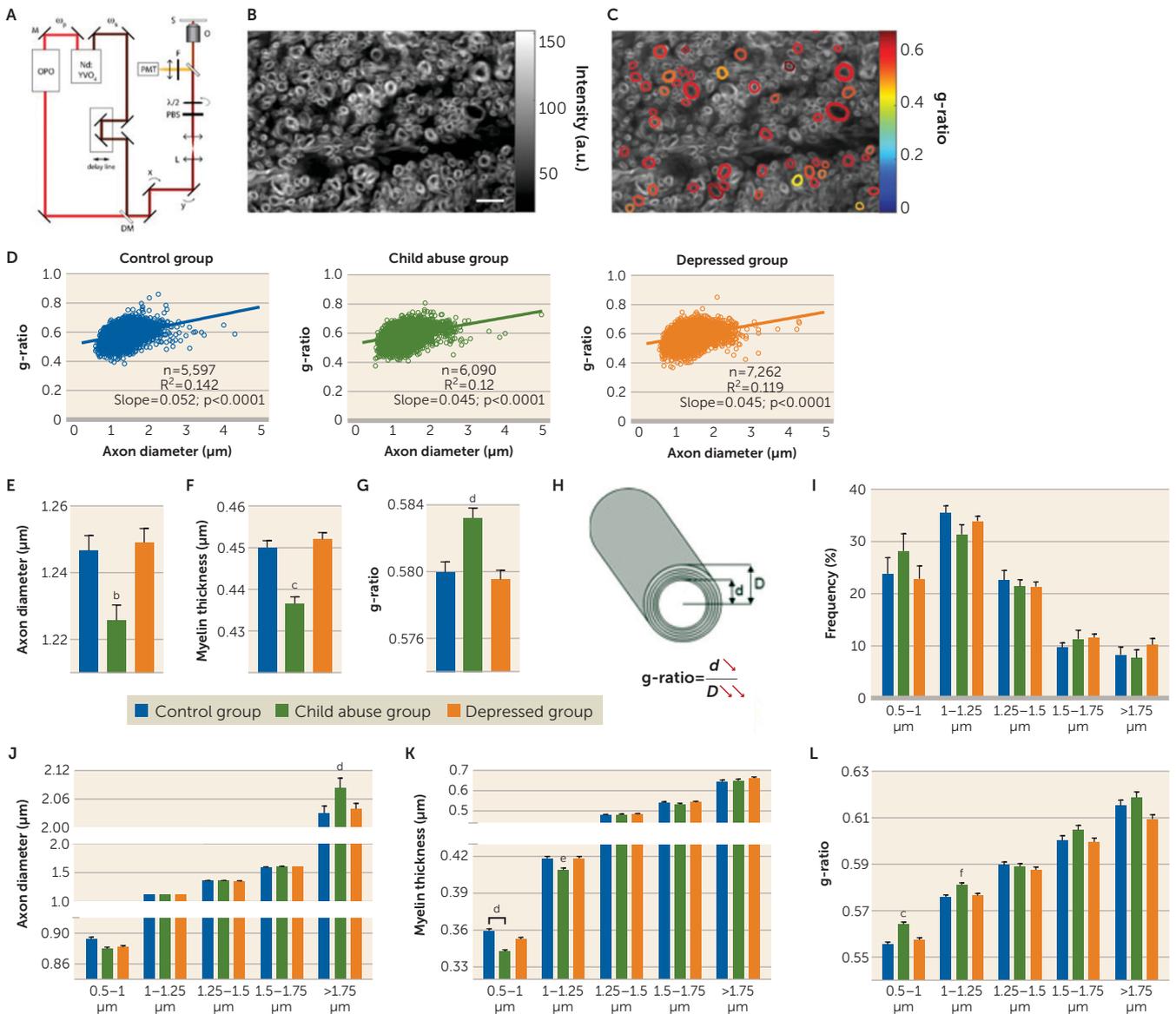
[a] Panel A is a schematic representation of the polarization-resolved coherent anti-Stokes Raman Scattering (CARS) setup. The fundamental Nd: YVO4 (brown) and OPO (red) signal-pulse trains are used as the Stokes ω_s and pump ω_p beams, respectively. The signal emitted from the sample (S) is collected in the epi direction (yellow). M=mirror; DM=dichroic mirror; L=lens; PBS=polarization beam splitter; $\lambda/2$=half-wave plate; O=objective lens; S=sample; F=anti-Stokes filter; PMT=photomultiplier tube. Panels B and C are images of myelinated fibers visualized by CARS microscopy before (panel B) and after (panel C) polarization-based segmentation. Myelin segments detected as oriented in the same plane (colored) are extracted for subsequent morphometric analysis. The scale bar is 8 μm. Panel D illustrates linear fits of g-ratio (defined as the ratio between the inner and outer diameters of the myelin sheath; see panel H) versus axon diameter of fibers detected by CARS of the control, child abuse, and depressed group. In panel E, the child abuse group showed an overall decrease in mean axonal diameter (one-way analysis of variance [ANOVA]: F=8.37, df=2, 18946, p<0.001; control group [N=5,597] versus child abuse group [N=6,090], p<0.01 by Tukey's honest significant difference; control group versus depressed group [N=7,262], p>0.05). In panel F, axons are less myelinated in the child abuse group (one-way ANOVA: F=27.05, df=2, 18946, p<0.0001; control group versus child abuse group, p<0.0001 by Tukey's honest significant difference; control group versus depressed group, p>0.05). In panel G, the mean g-ratio of cingulate cortex fibers is increased in the child abuse group (one-way ANOVA: F=11.68, df=2, 18946, p<0.0001; control group versus child abuse group, p<0.001 by Tukey's honest significant difference; control group versus depressed group, p>0.05). These effects could not be attributed to differences in age or quality of postmortem tissue, as these parameters did not affect axon diameter, myelin thickness, or g-ratios (see Figure S13 in the online data supplement). Panel H is a schematic representation of the effects of child abuse on myelinated axon morphometry. The g-ratio of cingulate cortex fibers is increased in the child abuse group (panels G and H) as a consequence of decreased axon diameter (panel E) and, to a greater extent, decreased myelin thickness (panel F). Panel I shows the distribution of cingulate cortex fibers based on their axonal diameter. No difference between groups was found in the frequency of fibers per category (two-way ANOVA, group effect F=1.056e-012, df=2, 155, p>0.05; class effect: F=93.23, df=4, 155, p<0.0001; interaction: F=1.156, df=8, 155, p>0.05) or in the number of fibers imaged per category and subject (see Figure S11 in the data supplement). In panel J, larger-caliber fibers (>1.75 μm) from the cingulate cortex show increased axon diameter in the child abuse group (two-way ANOVA, class-by-group interaction: F=11.41, df=8, 18934, p<0.0001; for fibers >1.75 μm: control group versus child abuse group, p<0.001 by Tukey's honest significant difference; control group versus depressed group, p>0.05). In panel K, small-caliber fibers (0.5–1 μm and 1–1.25 μm) are less myelinated in the child abuse

affect oligodendrocytes located in the cingulate cortex gray matter. Using FACS, we conducted the first analysis of DNA methylation in human oligodendrocytes and showed that cell type–specific epigenetic reprogramming may account, at least in part, for child abuse effects on myelin. Accordingly, for POU3F1 and LINGO3, the results indicated that DNA methylation levels were specifically decreased in oligodendrocytes, but not neurons. Oligodendrocyte-specific differential methylation of these two genes had no detectable effect on their transcriptional activity at the whole tissue level (RNA sequencing data). Because of the dynamic relationship between DNA methylation and gene expression during brain development (33), it is possible that these two adaptations represent epigenetic "traces" of child abuse that no longer have an impact on gene expression in adulthood.

Ultimately, we found that individuals abused during childhood showed decreased expression of a large collection of myelin-related genes in the cingulate cortex, suggesting a strong impairment in oligodendrocyte function. Strikingly, this global down-regulation was completely absent in depressed suicide completers with no history of child abuse, and it correlated nicely with gene expression changes observed in an animal model of unfavorable maternal care. Altogether, these results document the crucial role of early-life experiences in setting appropriate myelin genes' activity in the cingulate cortex. They also suggest a pathophysiological model whereby global cingulate cortex myelin down-regulation following a history of child abuse is not necessary for the emergence of depression. Rather, it may represent a neurobiological vulnerability that results from child abuse and potentiates the risk of psychopathology throughout life in affected individuals, thereby contributing to higher impulsive, aggressive, or anxiety traits and more frequent substance use and depressive disorders (3). Finally, an important question raised by these findings is whether myelin changes also occur in resilient individuals, that is, those who remain psychiatrically healthy despite adverse experiences in early life.

A limited number of postmortem studies on depression have reported transcriptional dysregulation of myelin-related genes in the temporal (34) and prefrontal cortices (35, 36). Of note, these studies were conducted in cohorts that were not characterized for early-life experiences of care and abuse. In the present work, depressive symptoms and suicide were not associated with any changes in the expression of myelin genes in a third brain structure, the cingulate cortex. Therefore, our findings highlight the need for further research to disentangle potential brain region–specific effects of child abuse and depression on myelin.

Recent preclinical evidence clearly supports the essential contribution of the quality of early-life experiences to cortical myelination. Accordingly, postweaning social isolation in rodents leads to decreased myelination in the frontal cortex (37, 38) that does not recover after social reintegration, indicating that myelination is critically regulated in early life by the social environment. Our own results are concordant with these findings and suggest that in humans, early-life experiences also have an impact on myelination, at least in the cingulate cortex. Because myelination has been shown to adapt to neuronal activity during motor learning (39), we speculate that this phenomenon may be similarly modulated in the social brain by the quality of life experiences. By threatening the development of healthy attachment patterns, early-life adversity may lastingly disrupt oligodendrocyte differentiation, cellular density, and transcriptional programming within the cingulate cortex, in part through epigenetic processes. Where in the brain, when during development, and how at the molecular level these effects are necessary and sufficient to have an impact on affective regulation cannot, by definition, be determined through human postmortem studies but hopefully will be explored in animal models by conducting time-controlled, brain region–specific manipulations of myelination. Ultimately, we propose that persistent myelin alterations induced in the cingulate cortex by child abuse may contribute to behavioral dysregulation and the emergence of interpersonal difficulties (40), thereby potentiating the risk of depression and suicide.

AUTHOR AND ARTICLE INFORMATION

From the McGill Group for Suicide Studies, Douglas Mental Health University Institute, McGill University, Montreal; Institut Universitaire en Santé Mentale de Québec, Quebec; Centre d'Optique, Photonique, et Laser, Université Laval, Quebec; Segal Cancer Centre, Lady Davis Institute, Jewish General Hospital, McGill University, Montreal; the Department of Psychiatry, McGill University, Montreal; the Sackler Program for Epigenetics and Psychobiology at McGill University and the Ludmer Centre for Neuroinformatics and Mental Health, Douglas Mental Health University Institute, McGill University, Montreal.

Address correspondence to Dr. Turecki (gustavo.turecki@mcgill.ca) and Dr. Mechawar (naguib.mechawar@mcgill.ca).

The first two authors contributed equally to this article.

group (two-way ANOVA, class-by-group interaction: F=2.904, df=8, 18934, p<0.01; 0.5- to 1-μm fibers: control group versus child abuse group, p<0.001; control group versus depressed group, p>0.05; 1- to 1.25-μm fibers: control group versus child abuse group, p<0.1; control group versus depressed group, p>0.1 by Tukey's honest significant difference). In panel L, small-caliber fibers have a higher g-ratio in the child abuse group (F=2.305, df=8, 18934, p<0.05; 0.5- to 1-μm fibers: control group versus child abuse group, p<0.0001; control group versus depressed group, p>0.05; 1- to 1.25-μm fibers: control group versus child abuse group, p<0.05; control group versus depressed group, p>0.05 by Tukey's honest significant difference). Finally, an increased molecular order of myelin was measured for all fibers, whatever their axonal diameter (see Figure S10 in the data supplement), which may reflect changes in the lipid composition and/or structural organization of myelin as a result of child abuse. Data in the bar graphs are presented as means, with error bars indicating standard error of the mean.
[b] Control versus child abuse group, Tukey's honest significant difference, p<0.01.
[c] Control versus child abuse group, Tukey's honest significant difference, p<0.0001.
[d] Control versus child abuse group, Tukey's honest significant difference, p<0.001.
[e] Control versus child abuse group, Tukey's honest significant difference, p<0.1.
[f] Control versus child abuse group, Tukey's honest significant difference, p<0.05.

REFERENCES

1. Teicher MH, Samson JA, Anderson CM, et al: The effects of childhood maltreatment on brain structure, function, and connectivity. Nat Rev Neurosci 2016; 17:652–666

2. Kendler KS, Kuhn J, Prescott CA: The interrelationship of neuroticism, sex, and stressful life events in the prediction of episodes of major depression. Am J Psychiatry 2004; 161:631–636

3. Turecki G: Dissecting the suicide phenotype: the role of impulsive-aggressive behaviours. J Psychiatry Neurosci 2005; 30:398–408

4. Wanner B, Vitaro F, Tremblay RE, et al: Childhood trajectories of anxiousness and disruptiveness explain the association between early-life adversity and attempted suicide. Psychol Med 2012; 42:2373–2382

5. Lutz PE, Turecki G: DNA methylation and childhood maltreatment: from animal models to human studies. Neuroscience 2014; 264:142–156

6. Peter CJ, Fischer LK, Kundakovic M, et al: DNA methylation signatures of early childhood malnutrition associated with impairments in attention and cognition. Biol Psychiatry 2016; 80:765–774

7. Labonté B, Suderman M, Maussion G, et al: Genome-wide epigenetic regulation by early-life trauma. Arch Gen Psychiatry 2012; 69:722–731

8. Trabzuni D, Ryten M, Walker R, et al: Quality control parameters on a large dataset of regionally dissected human control brains for whole genome expression studies. J Neurochem 2011; 119:275–282

9. Dumais A, Lesage AD, Alda M, et al: Risk factors for suicide completion in major depression: a case-control study of impulsive and aggressive behaviors in men. Am J Psychiatry 2005; 162:2116–2124

10. Bifulco A, Brown GW, Lillie A, et al: Memories of childhood neglect and abuse: corroboration in a series of sisters. J Child Psychol Psychiatry 1997; 38:365–374

11. Chen GG, Diallo AB, Poujol R, et al: BisQC: an operational pipeline for multiplexed bisulfite sequencing. BMC Genomics 2014; 15:290

12. Chen GG, Gross JA, Lutz PE, et al: Medium throughput bisulfite sequencing for accurate detection of 5-methylcytosine and 5-hydroxymethylcytosine. BMC Genomics 2017; 18:96

13. Subramanian A, Tamayo P, Mootha VK, et al: Gene set enrichment analysis: a knowledge-based approach for interpreting genome-wide expression profiles. Proc Natl Acad Sci USA 2005; 102:15545–15550

14. Bégin S, Dupont-Therrien O, Bélanger E, et al: Automated method for the segmentation and morphometry of nerve fibers in large-scale CARS images of spinal cord tissue. Biomed Opt Express 2014; 5:4145–4161

15. Koenigsknecht J, Landreth G: Microglial phagocytosis of fibrillar beta-amyloid through a beta1 integrin-dependent mechanism. J Neurosci 2004; 24:9838–9846

16. Mi S, Miller RH, Lee X, et al: LINGO-1 negatively regulates myelination by oligodendrocytes. Nat Neurosci 2005; 8:745–751

17. Ryu EJ, Wang JY, Le N, et al: Misexpression of Pou3f1 results in peripheral nerve hypomyelination and axonal loss. J Neurosci 2007; 27:11552–11559

18. Barros CS, Nguyen T, Spencer KS, et al: Beta1 integrins are required for normal CNS myelination and promote AKT-dependent myelin outgrowth. Development 2009; 136:2717–2724

19. Lein ES, Hawrylycz MJ, Ao N, et al: Genome-wide atlas of gene expression in the adult mouse brain. Nature 2007; 445:168–176

20. Milner R, Edwards G, Streuli C, et al: A role in migration for the alpha V beta 1 integrin expressed on oligodendrocyte precursors. J Neurosci 1996; 16:7240–7252

21. Meaney MJ, Szyf M: Maternal care as a model for experience-dependent chromatin plasticity? Trends Neurosci 2005; 28:456–463

22. Nishiyama A, Komitova M, Suzuki R, et al: Polydendrocytes (NG2 cells): multifunctional cells with lineage plasticity. Nat Rev Neurosci 2009; 10:9–22

23. Takada N, Kucenas S, Appel B: Sox10 is necessary for oligodendrocyte survival following axon wrapping. Glia 2010; 58:996–1006

24. Cai J, Zhu Q, Zheng K, et al: Co-localization of Nkx6.2 and Nkx2.2 homeodomain proteins in differentiated myelinating oligodendrocytes. Glia 2010; 58:458–468

25. Cleff C, Gasecka A, Ferrand P, et al: Direct imaging of molecular symmetry by coherent anti-Stokes Raman scattering. Nat Commun 2016; 7:11562

26. Perge JA, Niven JE, Mugnaini E, et al: Why do axons differ in caliber? J Neurosci 2012; 32:626–638

27. Innocenti GM, Vercelli A, Caminiti R: The diameter of cortical axons depends both on the area of origin and target. Cereb Cortex 2014; 24:2178–2188

28. Johansen-Berg H, Gutman DA, Behrens TE, et al: Anatomical connectivity of the subgenual cingulate region targeted with deep brain stimulation for treatment-resistant depression. Cereb Cortex 2008; 18:1374–1383

29. Bick J, Zhu T, Stamoulis C, et al: Effect of early institutionalization and foster care on long-term white matter development: a randomized clinical trial. JAMA Pediatr 2015; 169:211–219

30. Basser PJ: Inferring microstructural features and the physiological state of tissues from diffusion-weighted images. NMR Biomed 1995; 8:333–344

31. Stikov N, Campbell JS, Stroh T, et al: In vivo histology of the myelin g-ratio with magnetic resonance imaging. Neuroimage 2015; 118:397–405

32. Tomasi S, Caminiti R, Innocenti GM: Areal differences in diameter and length of corticofugal projections. Cereb Cortex 2012; 22:1463–1472

33. Baker-Andresen D, Ratnu VS, Bredy TW: Dynamic DNA methylation: a prime candidate for genomic metaplasticity and behavioral adaptation. Trends Neurosci 2013; 36:3–13

34. Aston C, Jiang L, Sokolov BP: Transcriptional profiling reveals evidence for signaling and oligodendroglial abnormalities in the temporal cortex from patients with major depressive disorder. Mol Psychiatry 2005; 10:309–322

35. Pantazatos SP, Huang YY, Rosoklija GB, et al: Whole-transcriptome brain expression and exon-usage profiling in major depression and suicide: evidence for altered glial, endothelial, and ATPase activity. Mol Psychiatry 2017; 22:760–773

36. Rajkowska G, Mahajan G, Maciag D, et al: Oligodendrocyte morphometry and expression of myelin-related mRNA in ventral prefrontal white matter in major depressive disorder. J Psychiatr Res 2015; 65:53–62

37. Makinodan M, Rosen KM, Ito S, et al: A critical period for social experience-dependent oligodendrocyte maturation and myelination. Science 2012; 337:1357–1360

38. Liu J, Dietz K, DeLoyht JM, et al: Impaired adult myelination in the prefrontal cortex of socially isolated mice. Nat Neurosci 2012; 15:1621–1623

39. Gibson EM, Purger D, Mount CW, et al: Neuronal activity promotes oligodendrogenesis and adaptive myelination in the mammalian brain. Science 2014; 344:1252304

40. Johnson JG, Cohen P, Gould MS, et al: Childhood adversities, interpersonal difficulties, and risk for suicide attempts during late adolescence and early adulthood. Arch Gen Psychiatry 2002; 59: 741–749